



# A parametric study on the dynamic lateral earth forces on retaining walls according to European and Turkish Building Earthquake Codes

Özgür Lütfi Ertuğrul <sup>\*1</sup>, Babür Bek Zahin <sup>1</sup>

<sup>1</sup>Mersin University, Civil Engineering Department, Türkiye

### Keywords

Seismic acceleration coefficient  
Soil friction angle  
Lateral earth forces  
Retaining Structures

### Research Article

DOI: 10.31127/tuje.1100015

Received: 07.04.2022

Accepted: 09.05.2022

Published: 31.08.2022

### Abstract

In the earthquake regulations of many countries, Mononobe-Okabe method was used to determine the seismic lateral earth forces and earth pressure coefficients for the design of retaining structures. However, there are various interpretation differences of this method between earthquake regulations of different countries. In this study, effect of different seismic acceleration coefficients ( $S_{DS}$ ) and different soil friction angles ( $\phi'_d$ ) on the seismic earth forces acting on a high retaining structure were investigated through a parametric study based on the methods described in 2018 Turkish Building Earthquake Code (TBEC-2018) and EuroCode-8 (EC-8). For this purpose, approximately 120 analyzes were carried out by using different parameters and the analysis results were shown in tables and figures. Analyses were performed for yielding rigid retaining walls and anchored walls for the principles defined in the mentioned earthquake codes. It was observed that the seismic lateral force estimations made with TBEC-2018 are higher compared to values calculated according to EuroCode-8. In the calculation of dynamic thrust, unexpected results may occur at some critical values of  $\theta$  angle which is dependent on the lateral acceleration coefficient.

## 1. Introduction

Earth retaining structures play an important role in the modern civil engineering infrastructure. In addition to static loads, additional earth forces can affect to the retaining walls during earthquakes. In order to design the retaining structures safely with the rules stipulated in different earthquake codes, dynamic loads created by earthquakes should be taken into account in addition to the static loads. However, due to the complicated nature of soils, it is very difficult to realistically predict the seismic behavior of the retaining structures and to perform an analysis with a loading method with many variables and many unknowns, such as seismic forces and soil inhomogeneity. Therefore, for the estimation of dynamic soil thrust forces, simplified models having different assumptions about soil, wall and ground acceleration should be made in order to be able to analyze the dynamics of the retaining structures under the seismic effect [1]. The effect of seismic loads on the retaining structures depends on the inertia of the structure, the behavior of the soil under the wall and the backfill, the characteristics of the seismic motion that

occur such as the amplitude and frequency of the dynamic load and the natural period of the retaining structure-backfill-foundation subsoil. Besides, retaining wall-soil interaction should be taken into account. Due to the earthquakes that occurred in 1923 in Japan and the collapse of many retaining walls after earthquakes, Okabe [2] and Mononobe- Matsuo [3] explained that the soil pressure can increase with the effect of earthquakes. So called “Mononobe-Okabe Method” is a refinement of the static Coulomb theory in quasi-static conditions. In the Mononobe-Okabe analysis which is basically recommended for dry cohesionless soils, the additional forces that occur due to the effect of horizontal and vertical accelerations in the Coulomb active or passive wedge are calculated and the force balance is rewritten accordingly to obtain the quasi-static soil force [4-5]. The Mononobe-Okabe method has been a reference point for quasi-static methods developed later, and has been included in many regulations including 2018 Turkey Building Earthquake Code (TBEC-2018) [6] and EuroCode8 – Chapter 5. For this reason, it is known that the formulas of TBEC-2018 and EC-8 Chapter 5 are very

\* Corresponding Author

(ertugrul@mersin.edu.tr) ORCID ID 0000-0002-1270-3649  
(baburbekzahin786@gmail.com) ORCID ID 0000-0001-8362-0667

Cite this article

Ertugrul, Ö. L., & Zahin, B. B. (2023). A parametric study on the dynamic lateral earth forces on retaining walls according to European and Turkish Building Earthquake Codes. Turkish Journal of Engineering, 7(3), 196-207

similar and the results obtained from the analyzes are in good harmony [7].

Eurocode 8 (2004) [8] regulation applies to European Union countries. In this regulation, an equivalent static method is proposed for the earthquake-proof design of retaining structures. With the publication of the (TBEC-2018), it has been observed that new sections have been added and many changes have been made in the section related to the retaining structures in the previous regulation on Buildings to be Constructed in Earthquake Zones (DBYH,2007) [9]. For the earth retaining structures, the calculation of horizontal and vertical static-equivalent earthquake coefficients is now being calculated according to the earthquake acceleration coefficients ( $S_{DS}$ ) which can be obtained from the new interactive earthquake map of Turkey. In addition, to obtain horizontal and vertical static-equivalent seismic coefficients, the earthquake acceleration coefficient ( $S_{DS}$ ) can be obtained from the Turkey Earthquake Map (TBEC-2018) which is currently available in [10].

## 2. Method

Previous Turkish Earthquake Code (TBEC-2007) classifies Turkey into different earthquake zones according to their seismicity and provides the necessary calculation, design and construction rules for the structures in these regions for stability, sufficient strength, durability, rigidity and ductility [11]. Similar philosophy of design is considered in new Turkey Building Earthquake Code 2018 however, earthquake zones approach is replaced with more realistic coordinate-based earthquake parameter maps. In earthquake codes that include earthquake engineering and its practical applications, it is known that structures are not damaged in small earthquakes, the damage to non-structural parts is accepted in medium-sized earthquakes, and structures are damaged beyond repair in large earthquakes, but they are prevented from complete collapse. According to the results obtained from new researches, necessary changes are made in earthquake regulations. The Turkish Earthquake Code has been updated and changed many times until now. In the Turkish Building Earthquake Regulation (TBEC-2018), which entered into force in 2018, it is foreseen that the dynamic soil thrust force will be calculated by the Mononobe-Okabe method. On the other hand, in TBEC-2018, the distributed loads, static and dynamic water forces are included in the calculations, and effect of vertical static-equivalent seismic coefficients ( $k_v$ ) in gravity direction should also be investigated. The largest of the two soil thrust forces found will give the soil thrust forces to be used in the design. Although the Mononobe-Okabe analysis indirectly indicates that the point on which the total active thrust acts is  $H/3$  above the base of the wall having height of  $H$ , empirical findings show that the point at which this force acts is higher under dynamic loading conditions. According to TBEC-2018 and EC-8 regulations, the application point of the resultant thrust force will be taken as the midpoint of the wall height ( $h=H/2$ ) for dynamic soil pressures. In this study, approximately 120 analyzes were performed in Excel

computer program by using different earthquake acceleration coefficients ( $S_{DS}$ ) and soil internal friction angle ( $\phi'_d$ ) based on the methods mentioned above for a parametric study. Analysis results are shown in tables and figures.

The terminology and flowchart used in the design of the retaining structures according to the 2018 Turkish Earthquake Code (TBEC-2018) and EuroCode 8 (EC-8), which are currently in force, are given in Figure 1 and Figure 2, respectively. In these forms;  $k_h$  and  $k_v$  are horizontal and vertical static-equivalent earthquake coefficient,  $S_{DS}$  is the design spectral acceleration coefficient (earthquake acceleration coefficient),  $r$  is the design coefficient,  $S_s$  is the map spectral acceleration coefficient for short period,  $F_s$  is the local ground effect coefficient,  $P_{water}$  and  $\Delta P_{water}$  are resultant static and dynamic water pressures,  $\theta$  is the angle (an angle that depends on horizontal and vertical earthquake coefficients.),  $\gamma^*$  is the soil unit weight,  $\gamma$  is the soil natural unit weight,  $\gamma_d$  is the saturated soil unit weight,  $\gamma_{water}$  is the water unit weight,  $d_{water}$  is the submerged height of the wall,  $\beta$  is the angle of inclination of the soil surface behind the wall with respect to the horizontal,  $\phi'_d$  is the design friction resistance angle of the soil (the angle of internal friction of the soil),  $\psi$  is the angle of the wall with respect to the horizontal (from the horizontal in front of the wall to the back of the wall),  $\delta_d$  is the angle of friction between the wall and the soil,  $K$  is the total (static+dynamic) earth pressure coefficient,  $K_a$  is the active earth pressure coefficient,  $K_p$  is the passive earth pressure coefficient,  $H$  is the wall height,  $q$  surcharge load,  $P_t$  is the total static force,  $P_s$  is the static and  $P_d$  is the dynamic force acting on retaining walls,  $\alpha$  is the ratio of design acceleration to gravitational acceleration,  $S$  is the soil factor,  $a_{vg}$  vertical component of design ground surface acceleration,  $a_g$  is the design ground surface acceleration,  $E_{ws}$  is the static water pressure,  $E_{wd}$  is the hydrodynamic water pressure,  $\gamma$  is the saturated soil unit volume weight,  $\gamma_{dry}$  is the dry unit weight of the soil,  $H_w$  is the height of the submerged wall,  $\gamma_\phi$  is a coefficient for the backfill soil,  $E_t$  is the total static force,  $E_s$  is the static force and  $E_d$  is the dynamic soil thrust acting on the retaining walls. Values of the soil parameters are given in Table 1. A simplified drawing is provided in Figure 3 to depict the angles and the forces acting on the gravity retaining wall.

## 3. Parametric Analyses

Considering the soil parameters given above, anchored and gravity-type earth retaining structures that can allow displacements were analyzed using the Excel computer program according to the methodology proposed by the TBEC-2018 and EC-8 Regulations.

Obtained static and dynamic thrust forces are summarized in Table 2 to Table 5. Results show that internal friction angle of the soil,  $\phi'_d$ , is an important factor on the horizontal static and dynamic thrust forces acting on the wall. In these tables,  $K_{as}$  denotes the static lateral earth pressure coefficient,  $P_{as}$  denotes the static lateral force,  $K_{ad}$  is the dynamic lateral earth pressure coefficient,  $E_{ad}$  is the dynamic earth thrust calculated

according to EC-8 and  $P_{ad}$  is the dynamic earth thrust calculated according to TBEC-2018.

In addition, it is seen that the short period design spectral acceleration coefficients ( $S_{DS}$ ) and the  $\theta$  angle which is dependent on these coefficients are effective in

the static and dynamic active soil pressure coefficients and the horizontal static and dynamic active thrust forces acting on the wall. As the earthquake acceleration coefficient ( $S_{DS}$ ) values increase, the horizontal dynamic active thrust forces acting on the wall also increase.

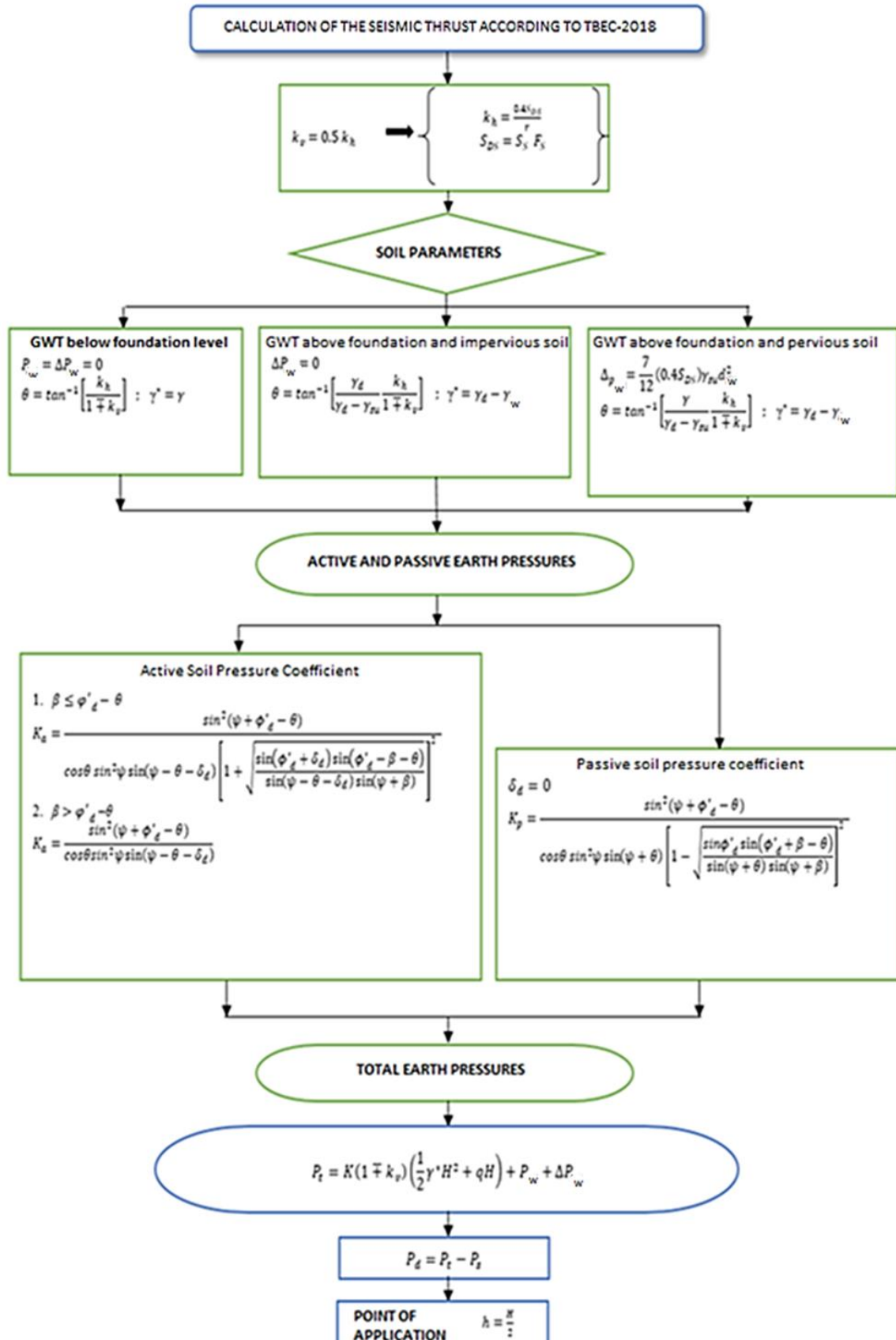


Figure 1. Design Schema according to TBEC-2018

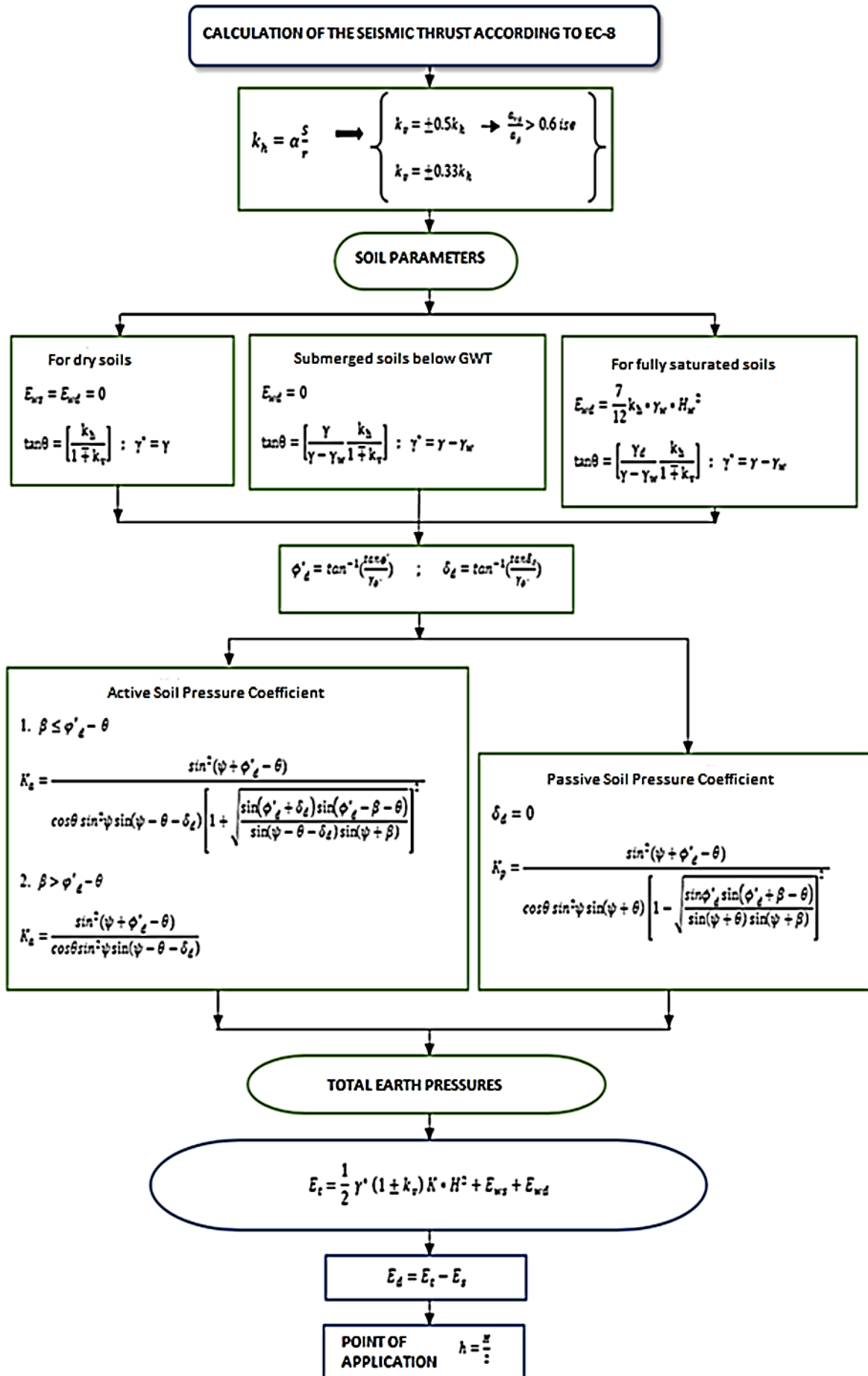
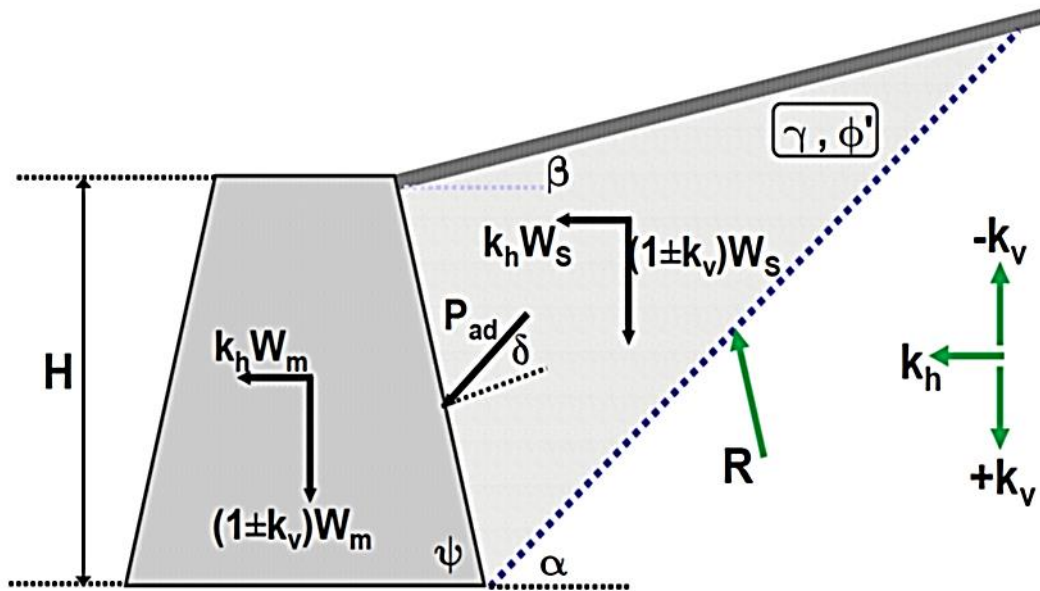


Figure 2. Design Schema according to EC-8

**Table 1.** Soil parameters

Explanation	Symbol	Value	Unit
Wall Height	$H$	12	$m$
Natural Unit Weight of Soil	$\gamma^*$	18	$kN/m^3$
Saturated Unit Weight of Soil	$\gamma_d$	21	$kN/m^3$
Unit weight of water	$\gamma_{water}$	10	$kN/m^3$
Surcharge load	$q_s$	-	$kN/m^2$
Angle of the wall surface with horizontal	$\psi$	90	$^\circ$
Internal angle of friction of the soil	$\varphi'_d$	20	$^\circ$
		30	$^\circ$
		40	$^\circ$
Friction angle between soil and wall	$\delta_d$	17	$^\circ$
Angle of the backfill surface with horizontal	$\beta$	0	$^\circ$
Angle of wall surface with vertical	$\theta^*$	-	$^\circ$
Permeability coefficient	$k_x$	$10^{-3}$	$m/sn$
Permeability coefficient (Impervious Soils)	$k_x$	$10^{-6}$	$m/sn$



**Figure 3.** A simplified drawing for the gravity retaining wall (Eurocode-8)

**Table 2.** A comparison of lateral dynamic earth pressures for anchored walls ( $r = 1$ ) with impermeable backfill

$\varphi'_d$	Static			Acceleration Coefficients				$\theta$	$K_{ad}$	$E_{ad}$ ( $kN/m$ )	$P_{ad}$ ( $kN/m$ )
	$K_{as}$	$P_{as}$ ( $kN/m$ )	$S_{DS}$			$\theta$					
				$k_h$	$k_v$						
20	0.431	558.387	0.5	0.2	0.1	22.989°	0.983	509.466	610.469		
			0.75	0.3	0.15	33.972°	1.372	715.579	847.811		
			1	0.4	0.2	43.668°	1.936	1001.523	1177.079		
			1.25	0.5	0.25	51.843°	2.805	1423.943	1663.503		
			1.5	0.6	0.3	58.571°	4.273	2109.681	2453.139		
30	0.299	388.072	0.5	0.2	0.1	22.989°	0.477	225.249	273.153		
			0.75	0.3	0.15	33.972°	1.606	954.859	1113.311		
			1	0.4	0.2	43.668°	2.365	1360.146	1580.004		
			1.25	0.5	0.25	51.843°	3.564	1966.983	2278.786		
			1.5	0.6	0.3	58.571°	5.636	2962.693	3425.361		
40	0.200	259.440	0.5	0.2	0.1	22.989°	0.329	177.429	210.509		
			0.75	0.3	0.15	33.972°	0.803	475.884	554.183		
			1	0.4	0.2	43.668°	2.610	1581.294	1827.079		
			1.25	0.5	0.25	51.843°	4.096	2352.169	2714.755		
			1.5	0.6	0.3	58.571°	6.7156	3634.415	4191.279		

**Table 3.** A comparison of lateral dynamic earth pressures for anchored walls ( $r = 1$ ) with permeable backfill

$\varphi'_d$	Static			Acceleration Coefficients			$\theta$	EC-8	TBEC-2018
	$K_{as}$	$P_{as}$ (kN/m)	$S_{DS}$			$K_{ad}$		$E_{ad}$ (kN/m)	$P_{ad}$ (kN/m)
				$k_h$	$k_v$				
20	0.431	558.387	0.5	0.2	0.1	19.983°	0.862	591.420	679.385
			0.75	0.3	0.15	30.008°	1.212	859.252	975.070
			1	0.4	0.2	39.289°	1.643	1151.698	1299.099
			1.25	0.5	0.25	47.489°	2.273	1527.839	1719.504
			1.5	0.6	0.3	54.513°	3.258	2050.489	2308.616
30	0.299	388.072	0.5	0.2	0.1	19.983°	0.361	310.336	345.677
			0.75	0.3	0.15	30.008°	1.394	1063.999	1200.805
			1	0.4	0.2	39.289°	1.968	1444.542	1626.278
			1.25	0.5	0.25	47.489°	2.826	1948.686	2194.079
			1.5	0.6	0.3	54.513°	4.198	2669.198	3011.033
40	0.200	259.440	0.5	0.2	0.1	19.983°	0.259	296.210	321.832
			0.75	0.3	0.15	30.008°	0.568	569.917	624.282
			1	0.4	0.2	39.289°	1.601	1277.591	1426.452
			1.25	0.5	0.25	47.489°	3.178	2226.991	2506.974
			1.5	0.6	0.3	54.513°	4.891	3127.126	3530.765

**4. Results**

In Figure 4 and Figure 5, variation of lateral seismic thrust versus  $S_{DS}$  values considering different soil internal friction angles for yielding type anchored walls and gravity walls are compared according to Euro Code 8 and 2018 Turkish Building Earthquake Code (TBEC-2018). Analyses were conducted for  $\varphi'_d = 20^\circ, 30^\circ, 40^\circ$ .

In the previous earthquake code, Turkey is classified into various seismic regions according to their seismicity and the active ground acceleration coefficient takes values between 0.1 and 0.4 according to these regions.

According to TBEC-2018,  $S_{DS}$  values can be estimated using the interactive earthquake maps. For this reason, in order to investigate the effect of the earthquake acceleration coefficient ( $S_{DS}$ ) on the dynamic thrust forces acting on the earth retaining structures, the variation of the earthquake acceleration coefficients and the dynamic thrust forces according to EC-8 and TBEC-2018 regulations are given in Figure 3 for the anchored walls and the gravity walls. It can be observed that lateral dynamic thrust increase as  $S_{DS}$  values increase. This increase is mostly linear for low soil internal friction angle values: On the other hand, the relationship between  $S_{DS}$  and  $P_{AD}$  becomes nonlinear for higher internal friction angle values. As seen in Figure 4, with the increase of earthquake acceleration coefficient ( $S_{DS}$ ), active dynamic thrust forces acting on the wall increase according to TBEC-2018 and EC-8 regulations.

The results obtained from both regulations (TBEC-2018 and EC-8) exhibits difference from each other. However, in both methods, with the increase of the soil internal friction angle ( $\varphi'_d$ ) the active dynamic thrust forces acting on the wall decrease. As can be seen from the figures, anchored walls ( $r=1$ ) are exposed to greater dynamic soil thrust forces than the gravity-type retaining structures ( $r=1.5$ ) with allowed displacements. With the increase of

earthquake acceleration coefficient ( $S_{DS}$ ) in dynamically impermeable soils, retaining structures are exposed to greater dynamic soil forces compared to permeable soils. Although additional dynamic water forces are taken into account in dynamically permeable soils, the water behind the wall flows towards the back of the wall and it is thought that the wall is less exposed to the water force. However, anchored walls ( $r=1$ ) are exposed to greater dynamic soil thrust forces than gravity-type yielding retaining structures ( $r=1.5$ ). The reason of this behavior can be considered as the limited displacements of the backfill soils due to the presence of ground anchors. The limited deformations in the soil does not let the soil strength to be fully mobilized. This will increase the lateral dynamic thrust acting on the retaining structure.

Figure 6 and Figure 7 depict the distribution of horizontal dynamic active thrust forces acting on the wall versus soil internal friction angle ( $\varphi'_d$ ) for different earthquake acceleration coefficients ( $S_{DS}=0.5, 0.75, 1, 1.25$  and  $1.5$ ) in anchored walls and gravity type walls according to Euro Code 8 and 2018 Turkish Earthquake Code.

As can be seen from these figures, with the decrease of the soil internal friction angle ( $\varphi'_d$ ), the active dynamic thrust forces acting on the wall increase according to TBEC-2018 and EC-8 regulations, and the results obtained from both regulations (TBEC-2018 and EC-8) are similar. The results obtained from the analyzes show that the anchored walls ( $r=1$ ) can be subjected to greater dynamic soil thrust forces than the gravity retaining structures ( $r=1.5$ ).

It is known that the soil internal friction angle ( $\varphi'_d$ ) has an inverse relationship with the horizontal thrust force acting on the wall. It is predicted that the horizontal thrust forces acting on the wall will decrease with the increase of the internal friction angle ( $\varphi'_d$ ) (Figure 6a, f and Figure 7a, b, g, h, i). Since different internal friction angles were used in the

parametric analyses, calculations were performed by using the formulas suggested for  $(\beta \leq \phi'_d - \theta)$  and  $(\beta > \phi'_d - \theta)$  cases according to EC-8 and TBEC-2018. With the increase of the internal friction angle ( $\phi'_d$ ), the horizontal thrust force acting on the wall increases up to a certain angle ( $\phi'_d$ ) and it is seen that the dynamic thrust forces decrease with the increase in the angle ( $\phi'_d$ ) which can be observed in Figure 6b, g, h and Figure 6c, d, f, j). However, only the second case  $(\beta > \phi'_d - \theta)$  formula is used in Figures 7c, d, e, i and Figure 7e. With the increase in the earthquake acceleration coefficient ( $S_{DS}$ ), the angle, which depends

Figure 6c, d, f, j). However, only the second case  $(\beta > \phi'_d - \theta)$  formula is used in Figures 7c, d, e, i and Figure 7e. With the increase in the earthquake acceleration coefficient ( $S_{DS}$ ), the angle, which depends

on the horizontal and vertical earthquake coefficients also increases. In calculating the value of the active soil pressure coefficient, the formula for

the first case  $(\beta \leq \phi'_d - \theta)$  does not yield results if the angle  $\theta$ , which depends on the horizontal and vertical earthquake coefficients, exceeds a certain soil internal friction angle.

Therefore, both regulations propose the formula for the second case  $(\beta > \phi'_d - \theta)$  to calculate active soil pressure. To be able to determine the active soil pressure, it is necessary to make calculations based on the second situation  $(\beta > \phi'_d - \theta)$  according to TBEC 2018 and EC-8, and there is a discrepancy between the results for the values where different formulas are being used. In other words, it was seen that use of the first and second formulas together in the calculation of the active soil pressure coefficient may cause numerical inconsistency thus affecting the results. This leads to the calculation of different dynamic earth pressure values, due to use of different formulas. This is found to be unrealistic and may be considered as a short coming of the TBEC-2018 procedure for the seismic design of the retaining walls.

**Table 4.** A comparison of lateral dynamic earth pressures for gravity walls ( $r = 1.5$ ) with impermeable backfill

$\phi'_d$ °	Static		$S_{DS}$	Acceleration Coefficients		$\theta$ °	EC-8			TBEC-2018	
	$K_{as}$	$P_{as}$ (kN/m)		$k_h$	$k_v$		$K_{ad}$	$E_{ad}$ (kN/m)	$P_{ad}$ (kN/m)		
20	0.431	558.387	0.5	0.133	0.067	15.255°	0.358	84.352	120.944		
			0.75	0.2	0.1	22.989°	0.983	509.466	610.469		
			1	0.267	0.133	30.431°	1.227	639.807	760.558		
			1.25	0.333	0.167	37.367°	1.536	800.017	945.043		
			1.5	0.4	0.2	43.668°	1.936	1001.523	1177.079		
30	0.299	388.072	0.5	0.133	0.067	15.255°	0.232	64.494	88.041		
			0.75	0.2	0.1	22.989°	0.477	225.249	273.153		
			1	0.267	0.133	30.431°	1.415	848.626	990.981		
			1.25	0.333	0.167	37.367°	1.825	1073.893	1250.379		
			1.5	0.4	0.2	43.668°	2.365	1360.146	1580.004		
40	0.200	259.440	0.5	0.133	0.067	15.255°	0.174	76.949	94.805		
			0.75	0.2	0.1	22.989°	0.329	177.429	210.509		
			1	0.267	0.133	30.431°	0.588	341.812	399.797		
			1.25	0.333	0.167	37.367°	1.163	700.529	812.866		
			1.5	0.4	0.2	43.668°	2.610	1581.294	1827.079		

**Table 5.** A comparison of lateral dynamic earth pressures for gravity walls ( $r = 1.5$ ) with permeable backfill

$\phi'_d$ °	Static		$S_{DS}$	Acceleration Coefficients		$\theta$ °	EC-8			TBEC-2018	
	$K_{as}$	$P_{as}$ (kN/m)		$k_h$	$k_v$		$K_{ad}$	$E_{ad}$ (kN/m)	$P_{ad}$ (kN/m)		
20	0.431	558.387	0.5	0.133	0.067	13.158°	0.275	191.359	218.709		
			0.75	0.2	0.1	19.984°	0.862	675.420	763.385		
			1	0.267	0.133	26.726°	1.097	886.448	993.659		
			1.25	0.333	0.167	33.207°	1.339	1089.760	1215.049		
			1.5	0.4	0.2	39.289°	1.643	1319.698	1467.099		
30	0.299	388.072	0.5	0.133	0.067	13.158°	0.187	199.747	218.332		
			0.75	0.2	0.1	19.984°	0.361	394.336	429.677		
			1	0.267	0.133	26.726°	0.704	696.786	765.226		
			1.25	0.333	0.167	33.207°	1.562	1320.548	1470.770		
			1.5	0.4	0.2	39.289°	1.968	1612.542	1794.278		
40	0.200	259.440	0.5	0.133	0.067	13.158°	0.142	221.662	235.988		
			0.75	0.2	0.1	19.984°	0.259	380.210	405.832		
			1	0.267	0.133	26.726°	0.438	574.742	617.111		
			1.25	0.333	0.167	33.207°	0.748	846.188	916.958		
			1.5	0.4	0.2	39.289°	1.601	1445.591	1594.452		

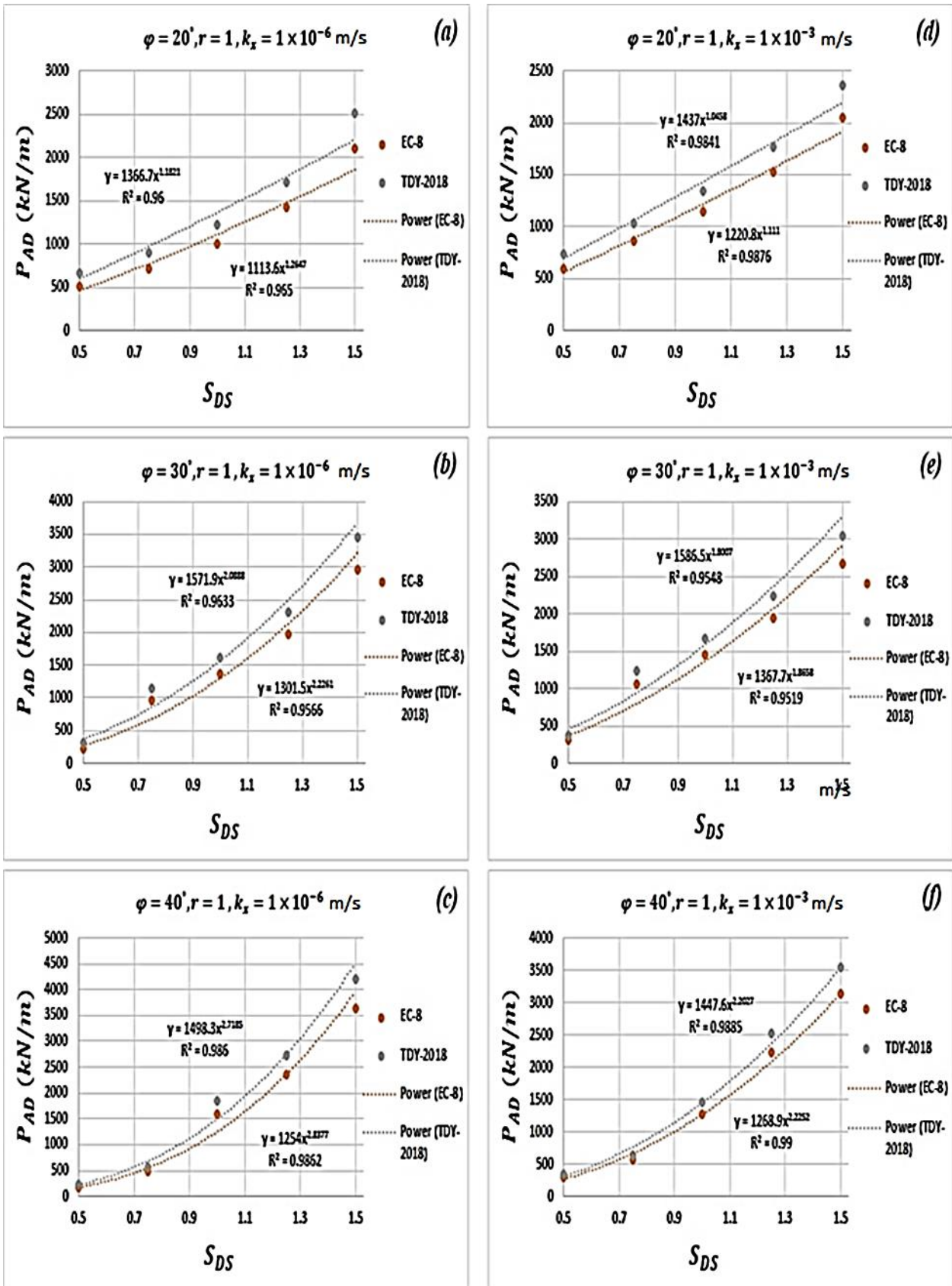


Figure 4. Variation of horizontal dynamic active thrust forces acting on the anchored wall with earthquake acceleration coefficient

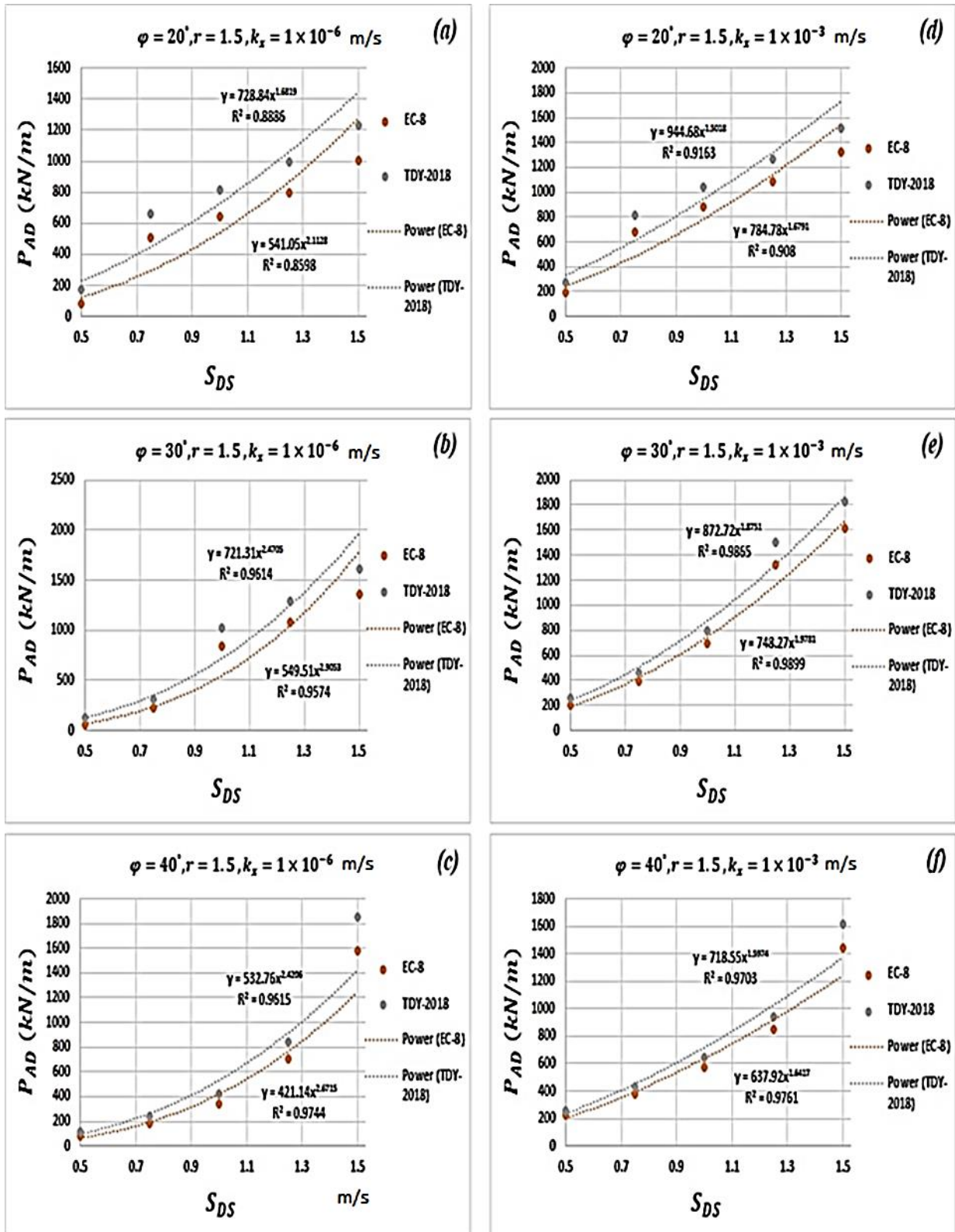


Figure 5. Variation of horizontal dynamic active thrust forces acting on the yielding gravity with the earthquake acceleration coefficient

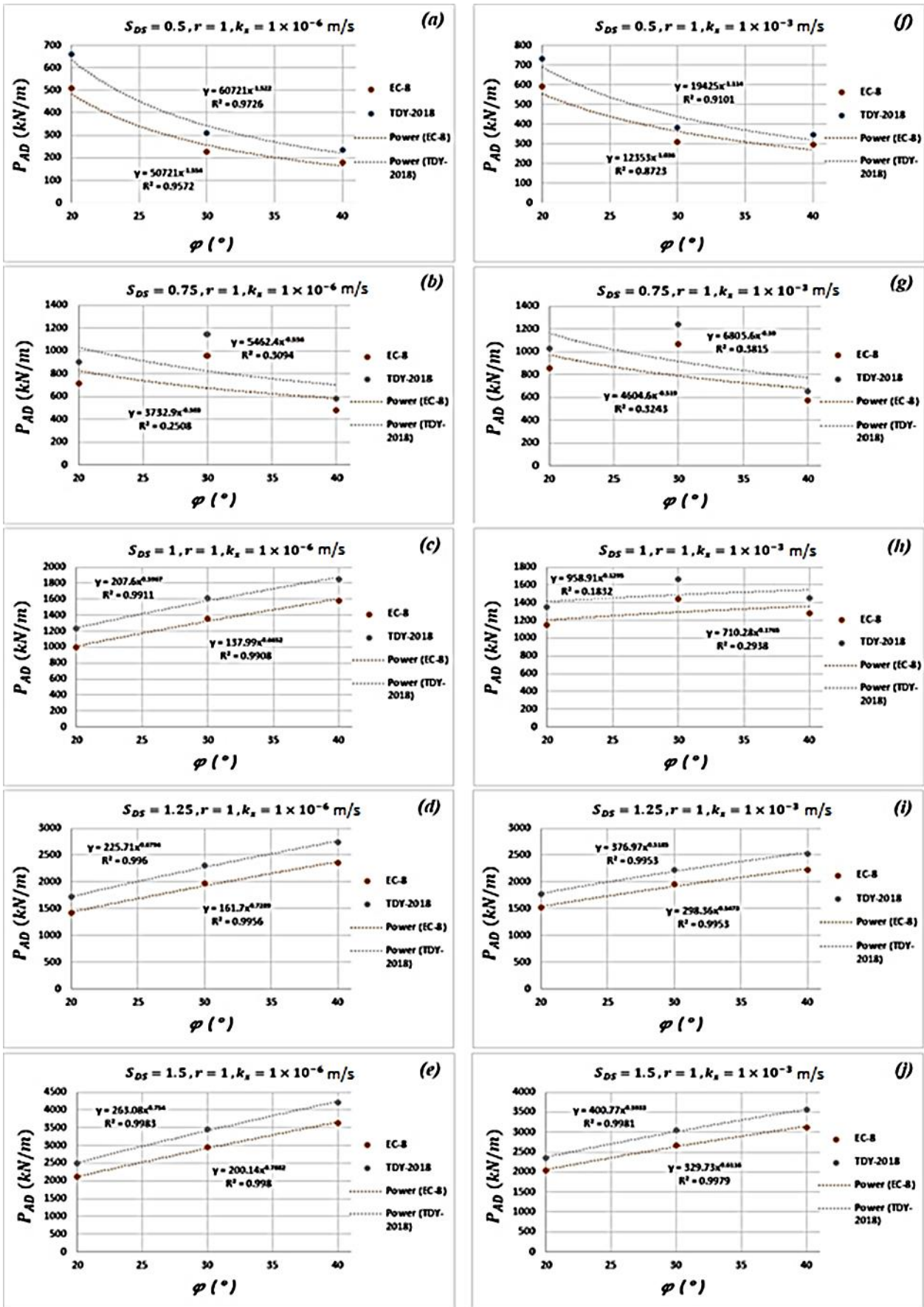


Figure 6. Variation of horizontal dynamic active thrust forces acting on the anchored wall with the internal friction angle of the soil ( $\phi'_d$ )

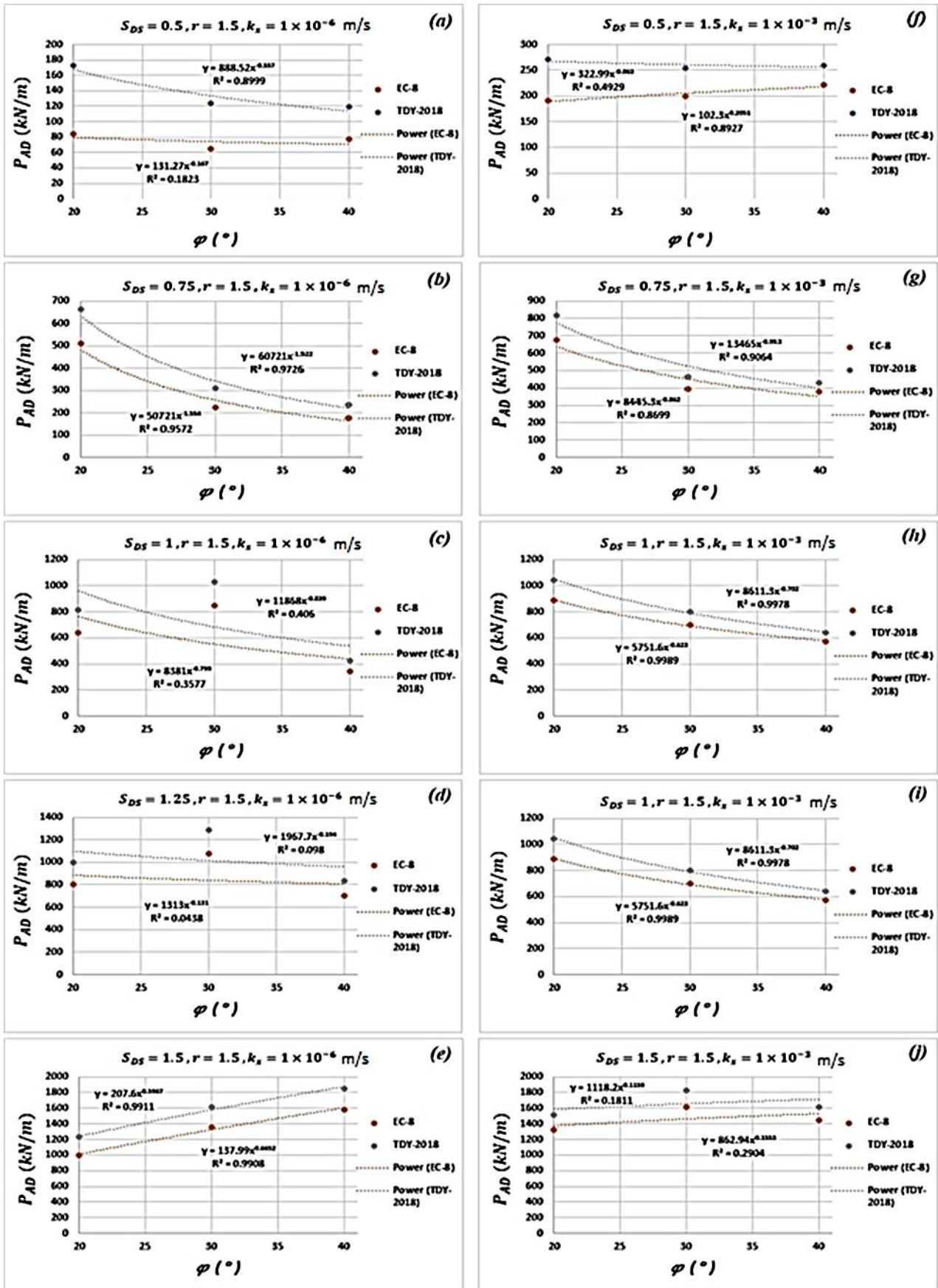


Figure 7. Variation of horizontal dynamic active thrust forces acting on the yielding gravity wall with the internal friction angle of the soil ( $\phi_0$ ) according to EC-8 and TBEC-2018 Regulations

## 5. Conclusion

Mononobe-Okabe method have generally been used to determine the dynamic lateral soil thrust and soil pressure coefficients for the design of retaining structures in various building earthquake codes. However, there are interpretation differences between these regulations in earthquake codes of different countries. In this study, seismic response of anchored walls and yielding gravity retaining walls are investigated according to the procedures suggested by Turkey Earthquake Code 2018 (TBEC-2018) and EuroCode-8 (EC-8). A parametric study was carried out using different earthquake acceleration coefficient ( $S_{DS}$ ) and different soil friction angles ( $\phi'_a$ ) for a 12 m high retaining wall. For this purpose, based on the procedures described in these earthquake codes, approximately 120 analyzes were performed using different parameters and the results of the analyses were shown in the form of tables and figures. The results show that the horizontal static and dynamic forces acting on the wall decrease with the increase of the soil internal friction angle ( $\phi'_a$ ). However, in cases where the angle  $\theta$ , which depends on the horizontal and vertical earthquake coefficient, is larger than the soil internal friction angle ( $\phi'_a$ ), dynamic active thrust forces acting on the wall increases with the increase in the soil internal friction angle for the cases ( $\theta > \phi'_a$ ). With the increase in the earthquake acceleration coefficient ( $S_{DS}$ ), active dynamic thrust forces increase according to the TBEC-2018 and EC-8 regulations, and the results obtained from both regulations are in agreement with each other. It is observed that the soil internal friction angle ( $\phi'_a$ ) and earthquake acceleration coefficients ( $S_{DS}$ ) are important factors due to their effect on the horizontal dynamic active thrust forces acting on the wall. According to EC-8 and TBEC-2018, the dynamic forces can take higher values than the static forces. It is known that the earth pressure coefficients used in TBEC-2018 and EC-8 regulations are based on Mononobe-Okabe method. However, in EC-8, it should be noted that the friction angle between the wall and the ground ( $\delta_a$ ) and the soil internal friction angle ( $\phi'_a$ ) values are reduced in the earth pressure calculations according to the equations given in Figure 2. As a further study, it is planned to suggest revised versions of the formulas to prevent illogical earth pressure calculations at critical values where different formulations are being used.

## Author contributions

**Özgür Lütfi Ertuğrul:** Conceptualization, Methodology, Reviewing and Editing, Validation.  
**Babur Bek Zahin:** Data curation, Software, Original draft preparation.

## Conflicts of interest

The authors declare no conflicts of interest.

## References

1. Bowles, L. E. (1996). *Foundation analysis and design*. New York: McGraw-Hill.
2. Okabe, S. (1926). General theory of earth pressures. J. Japan. Soc.Civil Eng., 12(1), 123-134.
3. Mononobe, N., & Matsuo, M. (1929). On the determination of earth pressures during earthquakes. Proc. World Engrg. Congress, 9, pp. 179-187.
4. Kramer, S. L. (1996). *Geotechnical earthquake engineering*. India: Pearson Education.
5. Das, B. M. and Sobhan, K. (2013). *Principles of geotechnical engineering*. USA: Cengage learning.
6. Türkiye Bina Deprem Yönetmeliği (TBDY). (2018). Ankara: Bakan İşleri Genel Müdürlüğü, Deprem Araştırma Dairesi.
7. Özberk, L. & Kahyaoğlu, M.R. (2018). Dayanma Yapılarının DBYBHY ve TBDY Gore Analiz Sonuçlarının Karşılaştırılması ve Tespitler. Zemin Mekaniği ve Geoteknik Mühendisliği, 17. Ulusal konferansı bildiri kitabı, 1-10. İstanbul
8. Eurocode-8. (2004). Design Of Structures For Earthquake Resistance Of Structures-Part 5: Foundations, Retaining Structures And Geotechnical Aspects. European Standard, European Committee for Standardization.
9. DBYBHY (2007). Deprem Bölgelerinde Yapılacak Binalar Hakkında Yönetmelik. Ankara: Çevre ve Şehircilik Bakanlığı.
10. <https://www.turkiye.gov.tr/afad-turkiye-deprem-tehlike-haritalari>
11. Gürsoy, Ş. (2013). İstinat Duvarlarına Etkiyen Aktif Zemin İtkilerinin Eurocode-8 ve Türkiye Deprem Yönetmeliğine Göre Karşılaştırılması. Karabük Üniversitesi, Gazi Üniversitesi Fen Bilimleri Dergisi, 1(4), 153-160.



© Author(s) 2023. This work is distributed under <https://creativecommons.org/licenses/by-sa/4.0/>